Validation of Intralaminar Behaviour of the Laminated Composites by Damage Mesomodel

Preetamkumar M. Mohite[1]
Indian Institute of Technology Kanpur, Kanpur, 208016, India

Gilles Lubineau[2] and Pierre Ladevèze[3]
LMT-Cachan (ENS-Cachan/Paris 6 univ./CNRS/UniverSud Paris), Cachan, 94231, France

and

Ana-Cristina Galucio[4]
EADS Innovation Works, Suresnes, France

In this article the enhanced version of the damage mesomodel (DML) developed at LMT is validated with the simulations performed for intralaminar damage mechanisms using User MATerial subroutines in Abaqus Standard. The damage mechanisms validated in the present study include fibre breaking, diffuse damage and matrix microcracking. The efficacy of the proposed model is shown by a series of identification results on industrial test cases for T700/M21 material. The basic identification tests include 0° traction and compression, traction on $[0_m/90_n]_S$ laminates, monotonic and cyclic traction of $[\pm 45]_{4S}$ and $[\pm 67.5]_{4S}$ laminates. The validation test is carried out for a 32-ply carbon-epoxy laminate with an open hole in traction. It is seen that DML is successful in predicting the initiation and propagation of the above mentioned intralaminar damage mechanisms.

I. Introduction

THE damage mesomodel is developed over last two decades at LMT-Cachan [1]. The damage mesomodel is based on three foundations: (i) mesoscale – the intermediate scale between the constituent level (micro) and structure (macro). Thus, the laminate is divided into two elementary components and which are continuous on the mesoscale: the ply [2] and the interface [3], (ii) damage indicators as internal variables which are constant through the thickness of a lamina and relate the effect of damage through the degradation of material elastic constants and (iii) the method of local states which relates thermodynamic forces to the strain energy of the damaged laminate.

The present DML is capable of characterizing the following intralaminar damage mechanisms: (i) fibre breaking, (ii) fibre matrix debonding (diffuse damage), (iii) matrix microcracking and (iv) plasticity effects. Further, it characterizes the interlaminar behaviour – delamination. However, the interest of the present work is limited to identification and validation by simulation of intralaminar damage mechanisms behaviour.

The attractive feature of the current DML is that there is a separate damage indicator for each of the intra and interlaminar damage mechanism. Further, it characterizes both initiation and propagation of these behaviours until final fracture.

The DML is refined in the past for various damage mechanism with micromechanical basis, especially for transverse microcracking and local delamination [4,5]. The refined model is compatible with the classical work of micromechanics in [6,7]. Further, the present DML has implemented with delay effects for localization and dynamic loading [8].

[1] Visiting Assistant Professor, Department of Aerospace Engineering, and Non Member
[2] Assistant Professor, LMT-ENS de Cachan, and Non Member
[3] Professor, LMT-ENS de Cachan, EADS Foundation Chair in "Advanced Computational Structural Mechanics" and Non Member
[4] Research Engineer, EADS Innovation Works, and Non Member

II. DML for Intralaminar Damage Behaviours

The details of the present DML are not presented in this paper. However, the complete DML including the above mentioned damage mechanisms and plasticity effects can be seen in [2] for ply behaviour and in [3] for the interlaminar behaviour. The present DML is an enhanced version of the basic DML [2], [3] with the addition of the micro-meso relationship based on homogenization for matrix microcracking and local delamination. The details of the micro-meso relationship can be seen in [4,5], [9-11].

The present DML has been implemented in commercial software Abaqus in the earlier works [9], [11]. The same has been used here for the identification and validation study.

III. DML Identification Tests and their Simulation

The main aim of the present paper is to identify and validate the present DML for the material T700/M21 for intralaminar damage mechanisms. The material is provided by EADS, IW. Further, the tests are also carried by them. The intralaminar damage mechanisms have been modeled as given in the above section and implemented in the commercial software Abaqus. In the following subsections we present the experimental and simulated results for the identification tests. The identification and verification of DML can also be seen in [12].

A. 0° Traction Test

The objective of this traction test is to characterize the ultimate failure load and the non-linearity with the increasing load. The figure 1(a) shows the longitudinal stress against the longitudinal strain and figure 1(b) shows the longitudinal stress against the transverse strain upto final fracture. From these figures it is clear that DML accurately captures the ultimate load for this material. Further, it captures the non-linearity during the loading. For this material the increase in the Young's modulus in longitudinal direction is about 20%.

B. 0° Compression Test

Again the aim of the present test is to validate the ultimate failure load and non-linear behaviour during the compression loading. The figure 2(a) shows the variation of the longitudinal stress v/s the longitudinal strain until final fracture of the specimen whereas, figure 2(b) shows the variation of the longitudinal stress v/s the transverse strain. The final fracture of the specimen and the non-linear behaviour is accurately predicted by the DML. Further, it should be noted that the final fracture of the specimen occurs earlier for the compression loading than the traction loading.

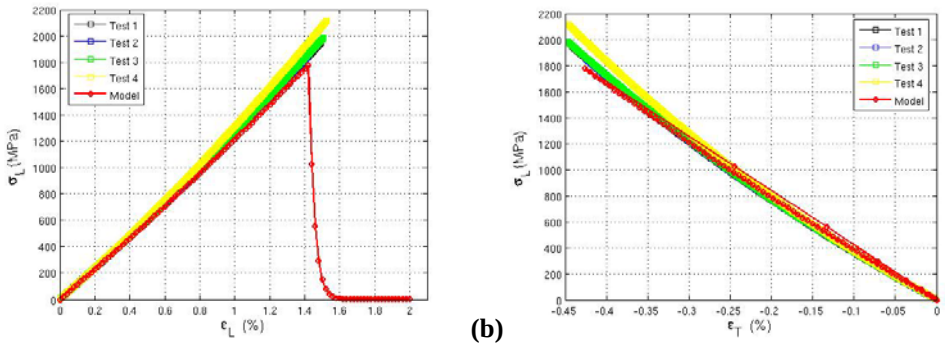

(a) (b)

Figure 1. Identification of fibre fracture in traction (a) variation of longitudinal stress vs longitudinal strain (b) variation of longitudinal stress vs transverse strain

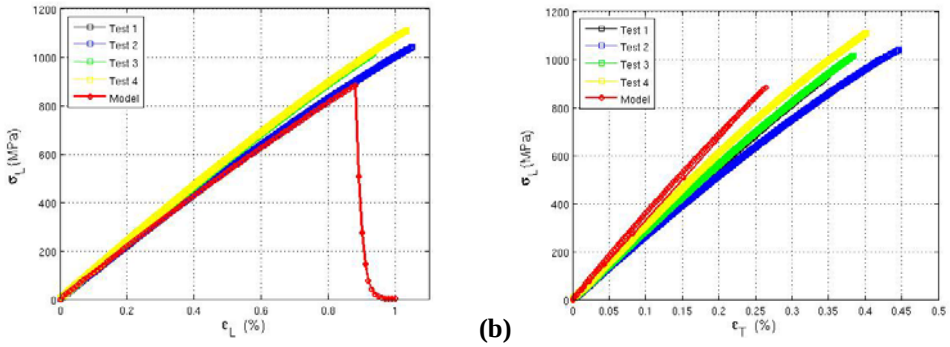

(a) (b)

Figure 2. Identification of fibre fracture in compression (a) variation of longitudinal stress vs longitudinal strain (b) variation of longitudinal stress vs transverse strain

C. $[0_m/90_n]_s$ Traction Test for Matrix Microcracking

Here, two laminate sequences – $[0_4/90_4/0_4]$ and $[0_4/90_{12}/0_4]$, are studied. The longitudinal mean stress at the first development of microcracking is validated along with its variation as the microcracking progresses. Further, the fibre breaking evolution along with longitudinal mean stress is also shown in figure 3(a) and (b). The longitudinal mean stress at which the microcracking develops is accurately predicted by the present mesomodel. Further, its variation with microcracking development is also in accordance with the experimental results. The specimen breaking occurs when the microcraking rate reaches a value of 0.5, both for experimental and simulated investigations.

The present DML provides more information for matrix microcraking and related morphology than the classical

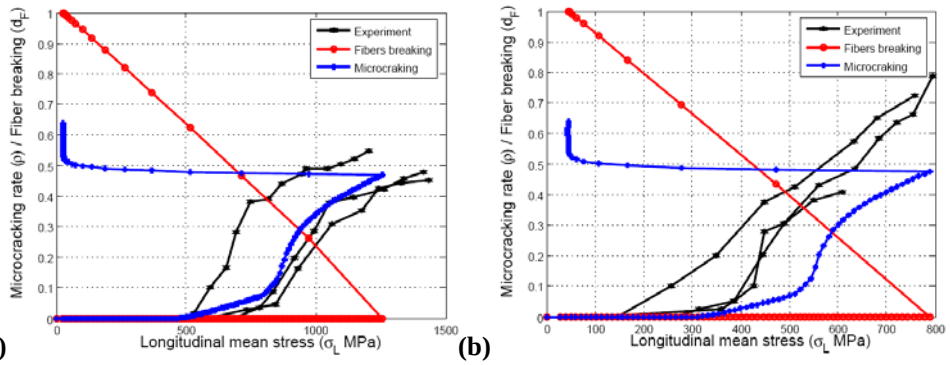

(a) (b)

Figure 3. Matrix microcraking identification in monotonic traction for (a) $[0_4/90_4/0_4]$ and (b) $[0_4/90_{12}/0_4]$ laminates.

damage approaches, for example see Ref. [13].

D. $[\pm45]_{4S}$ Cyclic Traction Test

Here, the monotonic cyclic traction test is carried out on $[\pm45]_{4S}$ laminate. Such a test is, in fact, a pure shear test. The present test is characterized by a large level of plasticity and very few microcracks towards the final breaking of the specimen. Further, diffuse damage is the main mechanism of damage (see Ref. [14]). The parameters validated in this validation study are: shear modulus and the plasticity parameters. The shear stress with shear strain variation is shown in figure 4(a). Here, it is to be noted that the model is valid for the first 5-6 load-unload cycles. The exploded view of the figure 4(a) is shown in figure 4(b). From this figure it is easy to see that the shear stress vs shear strain curve obtained overlaps the experimental one. The model does not account the large fibre rotations occurring after 5-6 load-unload cycles. Further, it should be noted that the isotropic hardening type plasticity model has been assumed for inelastic effects.

E. $[\pm 67.5]_{4S}$ Cyclic Traction Test

The plasticity parameters obtained in the previous test cases are also validated using the cyclic traction for this laminate sequence. This test is coupled transverse-shear loading case. For this laminate sequence, the plasticity effects are not as comparable to previous laminate sequence. The figure 5(a) shows curve for global longitudinal force vs global longitudinal strain. The curve obtained by the model is in accordance with the experimental results. The final fracture of the specimen is noted at the force value of 5500 *N* whereas the model predicts the failure at force value of 5700 *N*. Further, the figure 5(b) shows the variation of global longitudinal force vs microcracking rate. The microcracking develops at the experimental force value of 4400 *N* whereas the model predicts the initiation

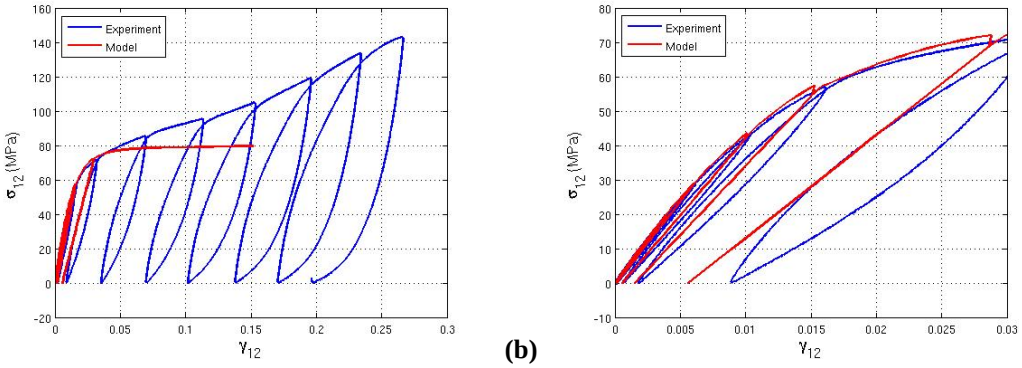

(a) **(b)**

Figure 4. Identification and validation of shear modulus, shear diffuse damage and plasticity parameters (a) shear stress vs shear strain (b) exploded view of (a) for $[\pm 45]_{4S}$ laminate.

of microcracking at the force value of 4700 *N*.

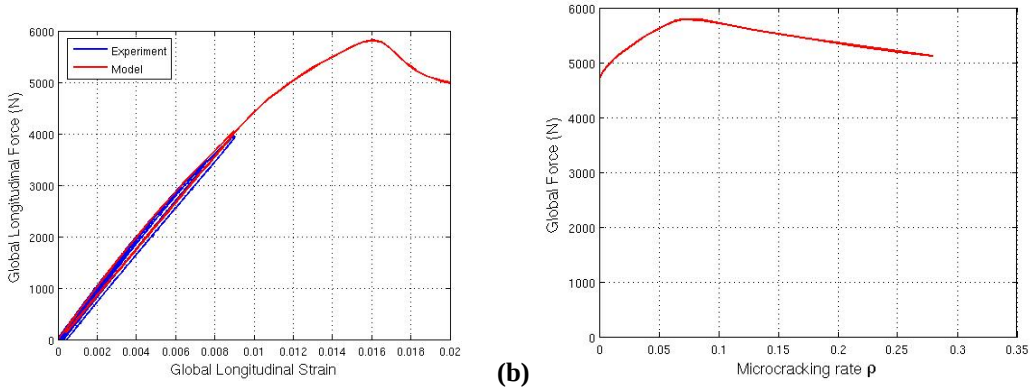

(a) **(b)**

Figure 5. Identification of (a) plasticity parameters in cyclic traction and (b) microcracking initiation in monotonic traction for $[\pm 67.5]_{4S}$ laminate.

IV. Validation of the DML for an Industrial Test Case

In this section, a 32 ply laminate of sequence $[0/-45/90_2/45/90_2/-45/90/45/90_2/-45/0/45/90]_S$ with an open central hole under monotonic traction is studied. Here, the half of the laminate in thickness direction has been modeled because of symmetry in the thickness direction. The 90^0 lamina at the centre is numbered as 0 through the 0^0 lamina at top is numbered as 12 for the simplicity of discussing the results. The 90_2 laminae are considered as a single lamina.

Here, 75% of fracture load is applied in traction to the specimen. The global fracture of the laminate occurs at 2.3 *mm* of displacement loading. All the results presented in this section are for this load-unload cycle. The fractured specimen is shown in figure 6(a) and (b).

A. Global Load Displacement Curve for Loading and Unloading

The global load-unload displacement curve is shown in figure 7. The load-unload displacement curve obtained by the present model is very close to the experimentally obtained curve. The initial deviation of the simulated curve

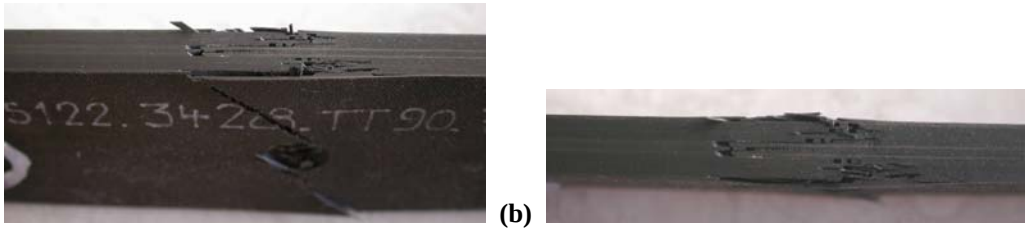

Figure 6. Fractured specimen of 32 ply laminate with an open hole under monotonic traction (Source: Centre D'Esaai Aéronautique de Toulouse).

is due to thermal residual effects considered for the matrix microcracking modeling.

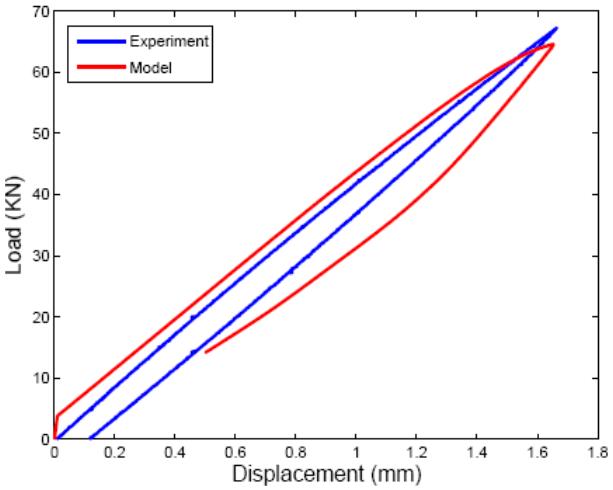

Figure 7. Global load-displacement curve for 75% of final fracture load.

B. Fibre Fracture

The damage maps for the fibre fracture in key laminae are shown in figure 8. Figure 8(a) shows the fibre breaking in 0^0 ply near the centre of the laminate (Ply No. 2). Figure 8(b) and (c) shows the fibre breaking in 45^0 (Ply No. 9) and -45^0 ply (Ply No. 11), respectively and (d) shows the fibre breaking in 0^0 ply at the top of the laminate. From figure 8(a), (d) and figure 6(a), (b) it can easily be seen that the present DML predicts the fibre breaking accurately. The fibre breaking in a ply has effect of ply orientation of the adjacent plies. The fibre breaking in all the laminae initiates from the edge of the open hole.

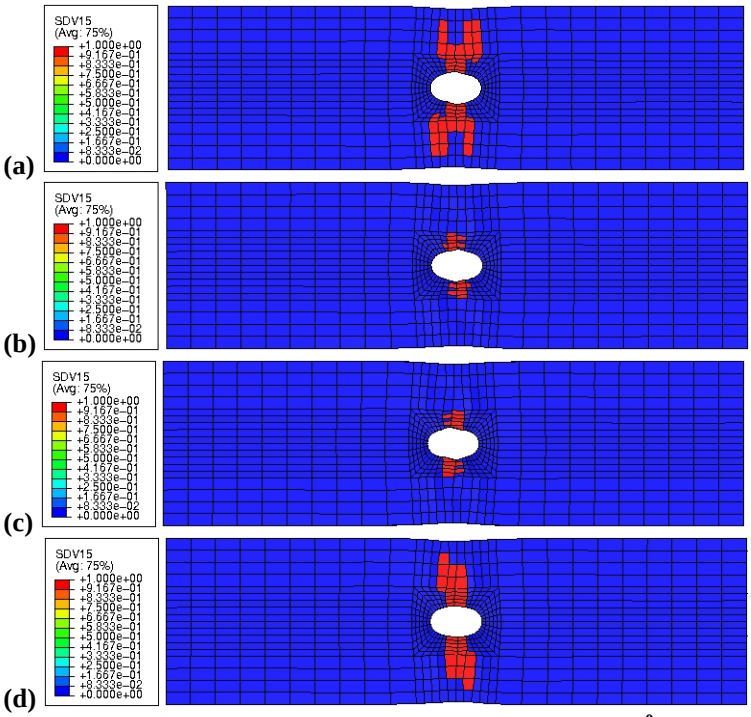

Figure 8. Validation for fibre breaking (a) Ply No. 2 (0^0 Ply), (b) Ply No. 9 (45^0 Ply) (c) Ply No. 11 (-45^0 Ply) and (d) Ply No. 12 (0^0 Ply).

C. Matrix Microcracking

The X-ray radiographs for matrix microcracking in 90^0 laminae and $\pm 45^0$ laminae are shown in figure 9(a) and (b), respectively. These X-ray radiographs are obtained at the 90% of fracture load. The damage maps for microcracking rate obtained by the model at the maximum load of 75% of fracture load are shown in figure 10 for some key laminae. Figure 10(a) and (b) shows the microcracking rate in 90^0 ply at the centre (Ply No. 0) and near to the top (Ply No. 10) of the laminate. Figure 10(c) and (d) shows the microcracking rate in 45^0 Ply (Ply No. 1), -45^0 Ply (Ply No. 3). From the figures it is easy to see that the microcracking in both 90^0 laminae and $\pm 45^0$ laminae are in exact accordance with the experimental results. The intensity of the microcracking and the area of microcracking are also in accordance with the experimental results of figure 9(a) and (b).

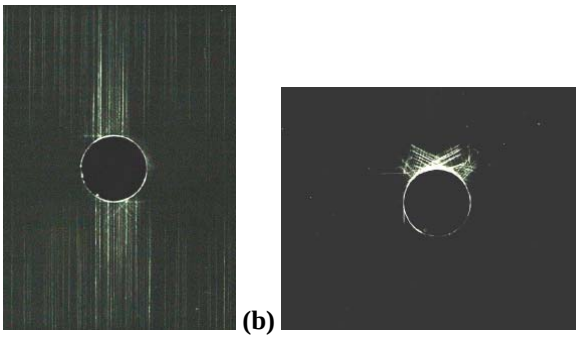

Figure 9. Experimental results for matrix microcracking in (a) 90° ply and (b) ±45° ply (Source: Centre D'Esaai Aéronautique de Toulouse).

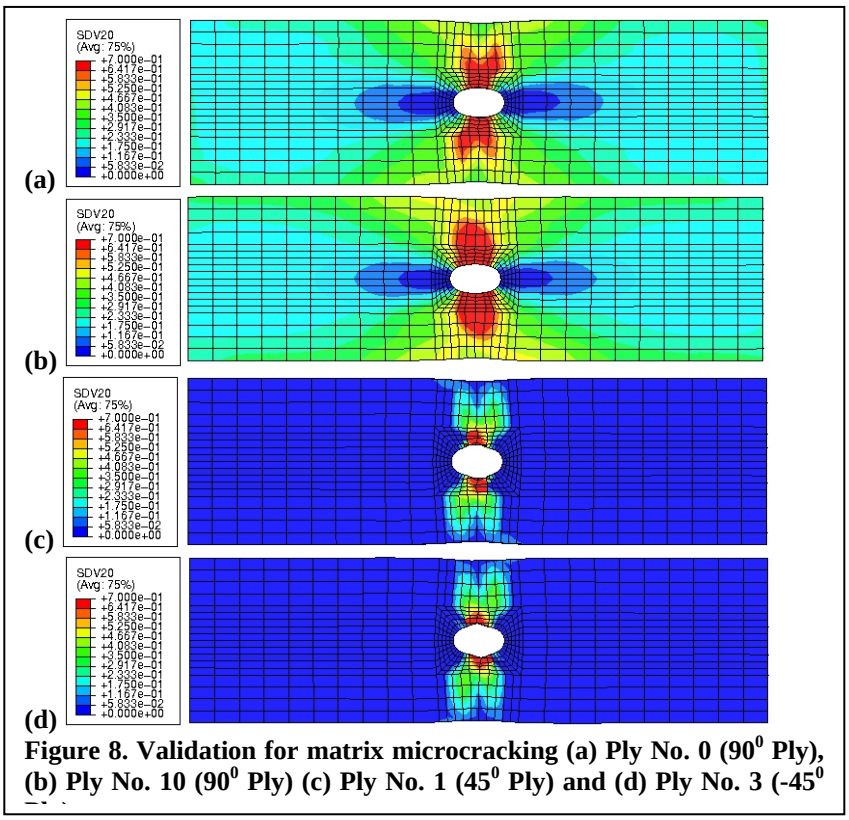

Figure 8. Validation for matrix microcracking (a) Ply No. 0 (90^0 Ply), (b) Ply No. 10 (90^0 Ply) (c) Ply No. 1 (45^0 Ply) and (d) Ply No. 3 (-45^0

V. Conclusion

The enhanced version of DML based on micro-meso relationship is previously implemented and illustrated in earlier works is validated for various industrial cases for the material T700/M21. The main conclusions of this study are enumerated as follows:

I. The traction and compression fracture behaviour of the fibres along with the non-linear behaviour is accurately captured by the present enhanced damage mesomodel.
II. The other identification tests for diffuse damage, matrix cracking and plasticity effects are also accurately predicted by DML.
III. The current model is very effective for the simulation of industrial cases of complex geometry and loading.

References

[1]Ladevèze P., "A damage computational method for composite structures", *Computers and Structures*, Vol. 44, 1992, pp. 79, 87.

[2]Ladevèze P., and Le Dantec E., "Damage modelling of the elementary ply for laminated composites", *Composite Science and Technology*, Vol. 43, 1992, pp. 257, 267.

[3]Allix O., and Ladevèze P., "Interlaminar interface modelling for the prediction of delamination", *Composite Structures*, Vol. 22, No. 4, 1992, pp. 235, 242.

[4]Ladevèze P., and Lubineau G., "On a damage mesomodel for laminates: micro-meso relationships, possibilities and limits", *Compos Science and Technology*, Vol. 61, No. 15, 2001, pp. 2149, 2158.

[5]Ladevèze P., Lubineau G., and Marsal D., "Towards a bridge between the micro- and the mesomechanics of delamination for laminated composites", *Composites Science and Technology*, Vol. 66, No. 6, 2006, pp. 698, 712.

[6]Nairn J., and Hu S., "Matrix microcracking. *In Talreja, editor, Damage* Mechanics of Composite Materials. 1994, pp. 187–243.

[7]Berthelot J. M., "Transverse cracking and delamination in cross-ply glass fiber and carbon-fiber reinforced plastic laminates: Static and fatigue loading", *Applied Mechanics Review*, Vol. 56, 2003, pp. 111, 147.

[8]Ladevèze P., Allix O., Deü J. F., and Lévêque D., "A mesomodel for localization and damage computation in laminates", *Computer Methods in Applied Mechanics and Engineering*, Vol. 183, 2000, pp. 105, 122.

[9]Lubineau G., and P. Ladevèze P., "Construction of a micromechanics-based intralaminar mesomodel and illustrations in ABAQUS/Standard", *Computational Material Science*, 2007, Article in Press, Available online.

[10]Lubineau G., "**A** pyramidal modelling scheme for laminates – identification of transverse cracking", *International Journal of Damage mechanics*, 2008, Submitted.
[11]Lubineau G., and Ladevèze P., "A pyramidal modeling for laminates composites – Illustrations Using Abaqus", 2008, *49th AIAA SDM/ASME/ASCE/AHS Conference*.
[12]Galucio A. C., Mohite P. M., Lubineau G., and Ladevèze P., "Validation on intralaminar behavior of the enhanced damage LMT-mesomodel", *13th European Conference on Composite Materials*, Switzerland, June 2008.
[13]Lapczyk I., and Hurtado J. A., "Progressive damage modeling in fiber reinforced materials", *Composites Part A*, Vol. 38, 2007, pp. 2333, 2341.
[14]Lagattu, F., and Lafarie-Frenot M., "Variation of PEEK matrix crystallinity in APC-2 composite subjected to large shearing deformation", *Composite Science and Technology*". Vol. 60, 2000, pp. 605, 612.